Front. Phys., 2011, 6(2): 224–230
DOI 10.1007/s11467-011-0170-7

RESEARCH ARTICLE

Metal-decorated defective BN nanosheets as hydrogen storage materials

Ming LI (李明)[1,2], **Ya-fei LI** (李亚飞)[2], **Zhen ZHOU** (周震)[2,†], **Pan-wen SHEN** (申泮文)[2]

[1] *College of Chemical Engineering and Biological Technology, Hebei Polytechnic University, Tangshan 063009, China*

[2] *Institute of New Energy Material Chemistry, Key Laboratory of Advanced Energy Materials Chemistry (Ministry of Education), Nankai University, Tianjin 300071, China*

E-mail: † *zhouzhen@nankai.edu.cn*

Received October 28, 2010; accepted December 20, 2010

Density functional theory computations were performed to investigate hydrogen adsorption in metal-decorated defective BN nanosheets. The binding energies of Ca and Sc on pristine BN nanosheets are much lower than the corresponding cohesive energies of the bulk metals; however, B vacancies in BN nanosheets enhance the binding of Ca and Sc atoms dramatically and avoid the clustering of the metal atoms on the surface of BN nanosheets. Ca and Sc strongly bind to defective BN nanosheets due to charge transfer between metal atoms and BN nanosheets. Sc-decorated BN nanosheets with B vacancies demonstrate promising hydrogen adsorption performances with a hydrogen adsorption energy of $-0.19 \sim -0.35$ eV/H_2.

Keywords BN, nanosheets, hydrogen storage, first principles

PACS numbers 73.22.-f, 73.63.Fg, 78.66.Fd, 78.67.Ch

1 Introduction

At present, hydrogen has been widely regarded as a promising carbon-free renewable energy carrier [1–3]. Immense efforts have been made worldwide to find feasible hydrogen storage materials with high gravimetric and volumetric densities. To get hydrogen uptake and release at ambient conditions [4, 5], the binding energies of H_2 are estimated as 0.2–0.4 eV/H_2 [6], which is intermediate between physisorption and chemisorption. Carbon nanotubes have ever attracted much attention as candidates for high-capacity hydrogen storage materials, due to the hollow tubular structure and large surface area. However, according to abundant investigations, pure carbon nanotubes exhibit low hydrogen storage potential [7, 8]. Metal-decorated carbon nanostructures have been proposed to achieve prospective hydrogen storage capacity [9–11].

Boron nitride (BN) nanotubes [12–18] have many analogical aspects with carbon nanotubes. In addition, in terms of the chemical and thermal stability, BN nanostructures may be stable lightweight hydrogen storage media. However, theoretical studies also disclose that pristine BN nanomaterials cannot serve as practical hydrogen storage materials at ambient conditions in view of the low hydrogen adsorption energy and gravimetric density [19, 20]. It was reported that BN nanotubes can take up 1.8–2.6 wt% hydrogen under ∼10 MPa at room temperature [21] and that the collapsed BN nanotubes prepared through metal-catalyzed growth mechanism exhibited a higher hydrogen storage capacity up to 4.2 wt% at ∼10 MPa [22]. The large hydrogen uptake in BN nanotubes was attributed primarily to chemisorption. The collapsed surfaces of BN nanotubes effectively increase the hydrogen adsorption capacity due to the increase of dangling bonds and specific surface area [23]. The enhanced hydrogen physisorption and chemsorption may also be attributed to interstitial regions in realistic nanotube bundles [24, 25]. Another reasonable possibility is that there remain metal cluster contaminants in BN nanotubes [26–28], and the enhanced hydrogen dissociation and adsorption may result from the strong interaction between metal atoms and hydrogen molecules. However, metal atoms tend to form clusters on the surface of nanomaterials due to the larger cohesive energy, and clustering reduces the hydrogen storage capacity and changes the hydrogen adsorption state [29, 30]. To avoid the clustering problem, the interaction between metal atoms and the substrates should be enhanced by introducing chem-

©Higher Education Press and Springer-Verlag Berlin Heidelberg 2011

ically active sites; therefore, vacancy defects are effective to increase the metal binding characteristics.

Recently, much experimental progress has been made in the preparation of BN nanosheets [31–33], and extensive computations have been performed to explore their physical and chemical properties and potential applications [34–37]. As the analogue of graphene, BN monolayer nanosheets may also be applicable to hydrogen storage media. In this work, we performed detailed density functional theory (DFT) computations to gain an insight into the hydrogen adsorption in BN nanosheets.

2 Computational methods

All computations were carried out within the DFT framework by using the Vienna *ab initio* simulation package (VASP) [38]. The electron exchange correlation is treated within the generalized gradient approximation (GGA) with PW91 functional [39]. Also, local density approximation (LDA) with CA functional [40] was employed to evaluate the hydrogen molecule adsorption energies and compare with the GGA results, as previous studies showed that GGA usually underestimates the H_2 adsorption energy, whereas LDA overestimates the interaction [24, 41–43], and the real value may be located in the range between GGA and LDA results; therefore, GGA and LDA results are widely adopted to evaluate the range of the hydrogen adsorption energies before better methodologies appear. Meanwhile, the electron–ion interactions are modeled by the ultrasoft pseudopotentials [44]. The cutoff energy for the plane wave-basis expansion was chosen to be 360 eV, and the convergence threshold was set as 10^{-4} eV in energy and 10^{-3} eV/Å in force. As for simulating two-dimensional BN sheets, a 4×4 supercell was used. The Monkhorst–Pack k point $4 \times 4 \times 1$ was adopted for the system. The positions of all the atoms in the supercell were fully relaxed during the geometry optimization.

The hydrogen adsorption energy, E_a, is defined as $E_a = [E_{(\mathrm{BNNS}+n\mathrm{H_2})} - E_{\mathrm{BNNS}} - nE_{\mathrm{H_2}}]/n$, where $E_{(\mathrm{BNNS}+n\mathrm{H_2})}$, E_{BNNS}, and $E_{\mathrm{H_2}}$ is the energy of the complex of BN nanosheets and hydrogen molecules, the separate BN nanosheets, and H_2 molecule, respectively. n is the number of hydrogen molecules absorbed.

3 Results and discussion

3.1 Ca and Sc adsorption on pristine BN nanosheets

Since H_2 is weakly adsorbed onto BN nanosheet [19], we attempted to introduce Ca and Sc atoms to BN nanosheets in order to increase the hydrogen adsorption energy (Fig. 1). The computed binding energies of Ca and Sc atom on pristine BN nanosheets, and the cohesive energies of bulk Ca and Sc metals are summarized in Table 1. After full relaxation, the distance between the Ca atom and the B or N atoms of the hexagon ring in pristine BN nanosheets is about 4.13 Å. The binding energy of Ca on pristine BN nanosheets is only 0.15 eV, which is even lower than that of Ca on pristine graphene [45]. The cohesive energy of the Ca bulk metal is 1.94 eV/Ca atom; therefore, Ca atoms definitely tend to form clusters on the surface of pristine BN nanosheets. Subsequently, the binding state of Sc atoms on pristine BN nanosheets was also examined. The distance between the Sc atom and the B or N atoms of the hexagon ring is about 2.68 Å in the optimized structure, and the binding energy of Sc on pristine BN nanosheets is 1.84 eV, which is much larger than that of Ca on BN nanosheets, but it is still lower than the cohesive energy of the Sc bulk metal (4.13 eV/Sc atom). Similar to Ca atoms, it is inevitable for Sc atoms to agglomerate on the surface of pristine BN nanosheets. To avoid the clustering problem, the binding states between metal atoms and BN nanosheets should be enhanced by introducing defects.

Table 1 Cohesive energies (E_c) of the bulk metals (Ca and Sc), average binding energies of metal atoms on pristine BN nanosheet (E_p), BN nanosheet with boron vacancy (E_{vb}), and BN nanosheet with nitrogen vacancy (E_{vn}). All the values are computed at the GGA-PW91 level of theory.

Metal	E_c /eV	E_p /eV	E_{vb} /eV	E_{vn} /eV
Ca	1.94	0.15	6.99	0.94
Sc	4.13	1.84	11.29	2.35

3.2 Ca and Sc atom adsorption on BN nanosheets with vacancies

Next, we consider BN nanosheets with various vacancies, so we remove one boron or nitrogen atom from the BN

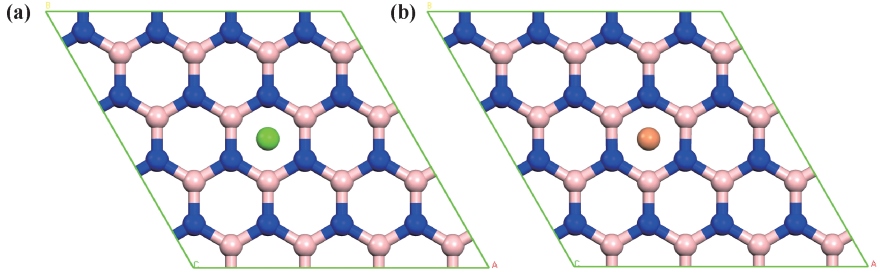


Fig. 1 Optimized structures of **(a)** one Ca atom adsorbed onto BN nanosheet and **(b)** one Sc atom adsorbed on BN nanosheet. B, N, Ca, and Sc are denoted with orange, blue, green, and brown balls, respectively.

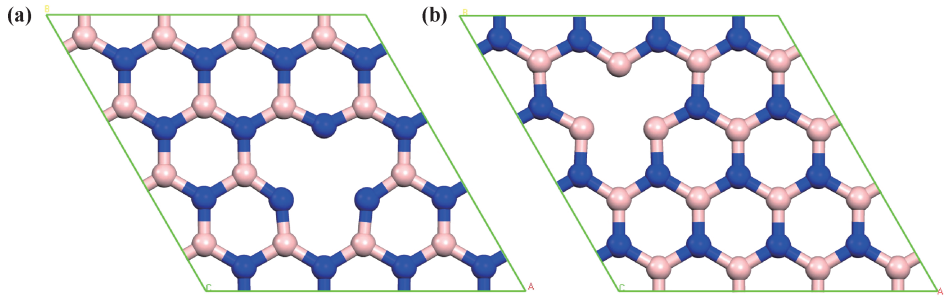


Fig. 2 Optimized structures of **(a)** one B vacancy and **(b)** one N vacancy created in BN nanosheets.

nanosheet to create a vacancy defect. Figure 2 is a schematic representation of the boron vacancy (V_B) and nitrogen vacancy (V_N) defect in BN nanosheets. After full relaxation, the distances between the three nitrogen atoms around the boron vacancy is 2.69 Å, which is larger than that in the pristine BN nanostructures (2.51 Å). The results are consistent with previous experimental and theoretical reports that the N–N distances are ∼2.70 Å surrounding boron vacancy and ∼2.50 Å in perfect BN nanostructures [46, 47]. There is a contraction in the distance between the boron atoms around the nitrogen vacancy (V_N) as compared with the pristine BN nanosheets, and the distance is about 2.35 Å, which is shorter than that in the pristine BN nanosheets (2.52 Å). The structural modification is important for the structural stability of B vacancy. Owning to the larger distance and the stronger repulsion of nitrogen atoms around boron vacancy, it is difficult to form chemical bonds among the nitrogen atoms around boron vacancy and get a pentagonal ring.

When we attached one Ca atom onto the nitrogen vacancy of BN nanosheet, as presented in Fig. 3(a), the optimized distance between the Ca atom and the three boron atoms around the nitrogen vacancy is 3.29 Å, and the binding energy between Ca and BN nanosheet with V_N is 0.95 eV, which is greatly enhanced as compared with that of pristine BN nanosheet. The increased binding energy is due to the larger charge transfer between metal atoms and BN substrate. The Hirshfeld charge analysis indicates that Ca carries a 0.34 |e| positive charge. However, the binding energy is still lower than the cohesive energy of the bulk Ca metal (1.94 eV), and Ca atoms persist in clustering on BN nanosheets with nitrogen vacancies. Similar results appeared when we introduced one Sc atom onto the nitrogen vacancy of BN nanosheet [Fig. 3(b)]. After full relaxation, the distance between the Sc atom and the three boron atoms around the nitrogen vacancy is 2.35 Å, and the binding energy is 2.35 eV, which is also lower than the cohesive energy of Sc bulk metal (4.13 eV). The Hirshfeld charge analysis indicates that 0.43 |e| charge is transferred from Sc atom to BN nanosheet with nitrogen vacancy. The smaller binding energy is unfavorable to exclude the formation of the clusters.

Then, we checked the effects of boron vacancies on the binding energies of metal atoms on BN nanosheets.

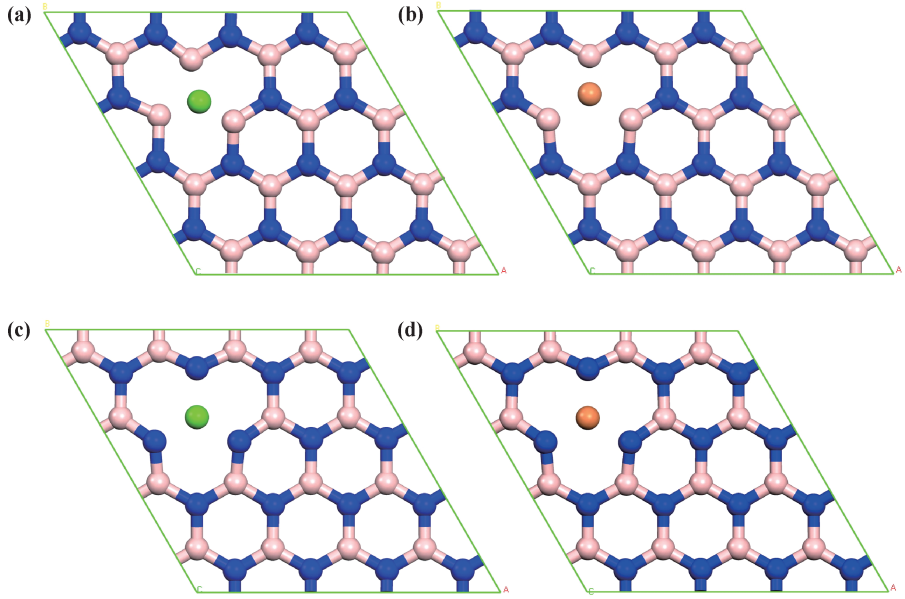


Fig. 3 Optimized structures of **(a)** one Ca atom added onto the nitrogen vacancy, **(b)** one Sc atom added onto the nitrogen vacancy, **(c)** one Ca atom added onto the boron vacancy, and **(d)** one Sc atom added onto the boron vacancy in BN nanosheets.

When we attached one Ca atom onto the boron vacancy of BN nanosheet, as shown in Fig. 3(c), the boron vacancy retains its structure, and no apparent distortion occurs. The effect of Ca on the vacancy structure is inconsistent with the case of graphene. Adding one Ca atom to the vacancy of graphene results in the formation of a 5–9 carbon ring [45]. After full relaxation, the distance between the Ca atom and the three nitrogen atoms around the boron vacancy is 2.17 Å. As listed in Table 1, the binding energy between Ca and the BN nanosheet with boron vacancy is 6.99 eV, which is increased so significantly as to exceed the cohesive energy of Ca bulk metal (1.94 eV). Ca atoms strongly bind to BN nanosheets due to charge transfer between metal atoms and BN substrate. We found that 0.73 |e| charge is transferred from Ca atom to BN nanosheet through Hirshfeld charge analysis. Similar results were obtained when we introduced one Sc atom onto the boron vacancy of BN nanosheet [Fig. 3(d)]. In the optimized structure, the distance between the Sc atom and the three nitrogen atoms around the boron vacancy is 1.98 Å, and the binding energy between Ca and vacancy is 11.29 eV, which is far larger than the cohesive energy of Sc bulk metal (4.13 eV). The Hirshfeld charge analysis shows that Sc carries a 0.71 |e| positive charge. As summarized in Table 1 and Fig. 4, lager binding energies are obtained in the cases of Ca and Sc adsorption in BN nanosheets with boron vacancies, accompanied by greater charge transfer. The larger binding energies are favorable to exclude the clustering problem.

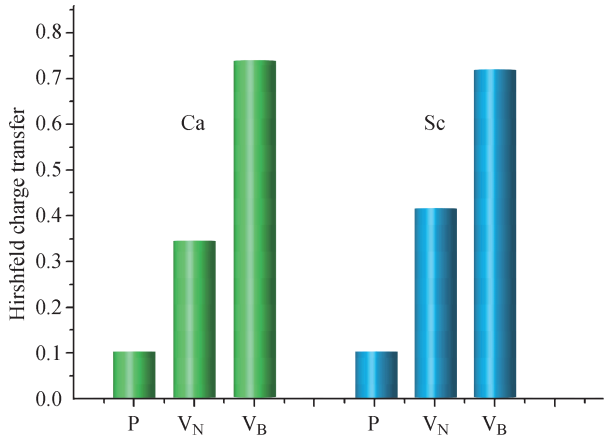


Fig. 4 Charge transfer of Ca and Sc atoms in pristine BN nanosheet and BN nanosheets with V_N or V_B.

The boron vacancies efficiently enhance the metal binding and dispersion. Recently, Iijima *et al.* have found abundant vacancy defects in the single layer of hexagonal BN prepared by means of controlled energetic electron irradiation, and they successfully validated that the predominant atomic defects are boron vacancies [47]. Since Ca and Sc atoms can bind tightly on BN nanosheets with V_B and avoid the clustering problems, metal-decorated BN nanosheets may be available experimentally and are promising hydrogen adsorption media.

The enhanced binding energies of transition metals at boron vacancy sites can be simply attributed to the more pronounced charge transfer; however, to get more insight, we have computed the density of states (DOS) for Sc-decorated pristine and defective BN nanosheets and compared with pristine and defective BN nanosheets. As shown in Fig. 5, pristine BN nanosheet is a typical semiconductor with a wide band gap. When an Sc atom is adsorbed on the BN nanosheet, the Fermi level is shifted into the conduction band, and new states appear around Fermi level. The partial DOS analysis demonstrates that these states are mainly from the Sc atom. The hybridization between Sc and BN nanosheet is found, but the 4s orbital of Sc atom is still occupied, which indicates that the hybridization between Sc and BN nanosheet is not strong. When a boron vacancy is introduced into BN nanosheet, an acceptor-like state appears near the Fermi level, which is mainly contributed by the N atoms around the vacancy site [N_{vacancy} in Fig. 5(c)]. Once Sc atom is bound, the above acceptor-like state disappears, and both 4s and 3d orbitals of Sc are unoccupied, indicating

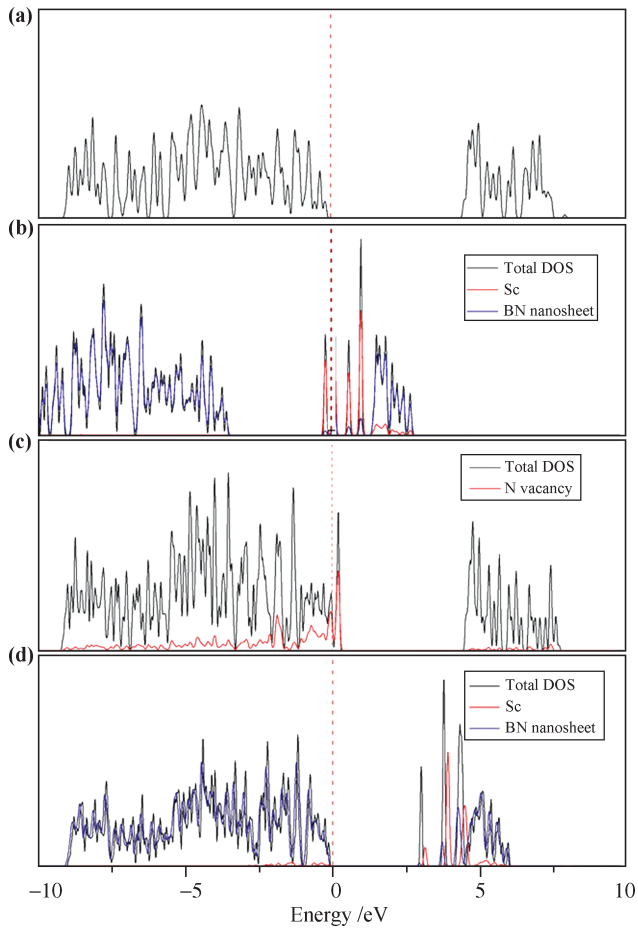


Fig. 5 Density of state (DOS) of **(a)** pristine BN nanosheet, **(b)** Sc-decorated BN nanosheet,**(c)** BN nanosheet with a boron vacancy, and **(d)** Sc-decorated BN nanosheet with a boron vacancy.

a strong hybridization between Sc atom and BN nanosheet, which can further explain the large binding energy of Sc atom in this case.

3.3 Hydrogen adsorption in metal-decorated BN nanosheets with vacancies

First, we checked the hydrogen adsorption on BN nanosheets with vacancies. We placed one hydrogen molecule onto the boron vacancy. After full relaxation, the dissociation of hydrogen molecule into hydrogen atoms is detected in the simulation. As shown in Fig. 6(a), molecular hydrogen is chemisorbed to boron vacancy; strong chemical bonds form between hydrogen and nitrogen atoms around the B vacancy. The bond length of N–H is 1.02 Å, and the binding energy is 5.32 eV/H_2. The whole dissociation process of hydrogen molecule is exothermic when introducing defects to BN nanosheets, in agreement with a previous report on BN nanotubes [48]. Similar results are obtained when we add hydrogen molecule onto the nitrogen vacancy, as depicted in Fig. 6(b). The hydrogen molecule is dissociated to form B–H bonds with the bond length of 1.20 Å, which is a little longer than that of N–H, and the binding energy is 0.88 eV/H_2. Chemisorption of hydrogen with large binding energies is unfavorable for the release of hydrogen at ambient conditions. In order to find the intermediate state between physisorption and chemisorption with a binding energy of 0.2–0.4 eV and achieve the reversible hydrogen uptake and release at ambient conditions, we then used Ca or Sc-decorated defective BN nanosheets to attach hydrogen molecules.

We investigated the interaction between Ca-decorated defective BN nanosheets and hydrogen molecules. As illustrated in Fig. 7, the equilibrium Ca–H bond length is about 2.55 Å. The H–H bond length is elongated to 0.76 Å (0.75 Å for isolated H_2) due to the interaction between Ca and H_2, and the binding energy is –0.1 eV/H_2 at the GGA level, which is smaller than those of many Ca decorated complexes [49–54]. The larger difference in electronegativity between nitrogen and boron leads to partially ionic bonding; therefore, the electronic structures of BN nanosheets and graphene differ apparently in spite of their isoelectronic nature. The polarized B–N bonds may account for the smaller binding energies. As more H_2 molecules approach Ca-decorated BN nanosheets with V_B, the average hydrogen adsorption energies, the distances between H_2 and Ca, and the H–H bond lengths change accordingly. The binding energy is slightly reduced from −0.10 eV to −0.07 eV at the GGA level, which may be due to the steric repulsion when the number of H_2 molecules increase. The H–H bond length is about 0.76 Å, and the average bond length between H_2 and Ca is about 2.66 Å. The adsorption energy is so weak that the hydrogen adsorption is in an unstable state at ambient conditions.

Next, we investigated the interaction between Sc-decorated defective BN nanosheets and hydrogen molecules. Hydrogen molecule is adsorbed with an elongated bond of 0.76 Å, and the bond length of Sc–H is 2.47 Å. The hydrogen adsorption energy is –0.19 eV/H_2 for GGA and –0.35 eV/H_2 for LDA. Such optimal molecular hydrogen binding energies make hydrogen adsorption and desorption feasible at ambient conditions, which is critical for practical applications. H_2 nondissociative binding to Sc-decorated BN nanosheets with V_B presents

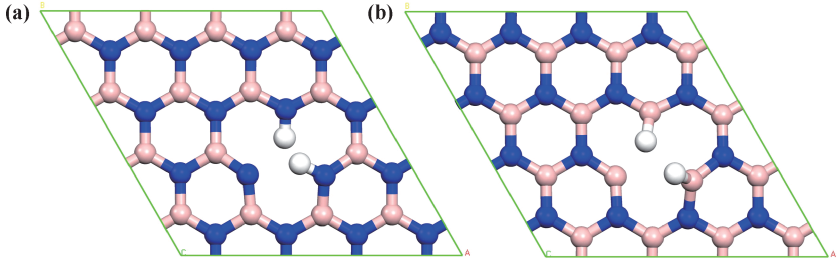


Fig. 6 Optimized structures of **(a)** one H_2 added onto the boron vacancy and **(b)** one H_2 atom added onto the nitrogen vacancy in BN nanosheets. H atoms are denoted with white balls.

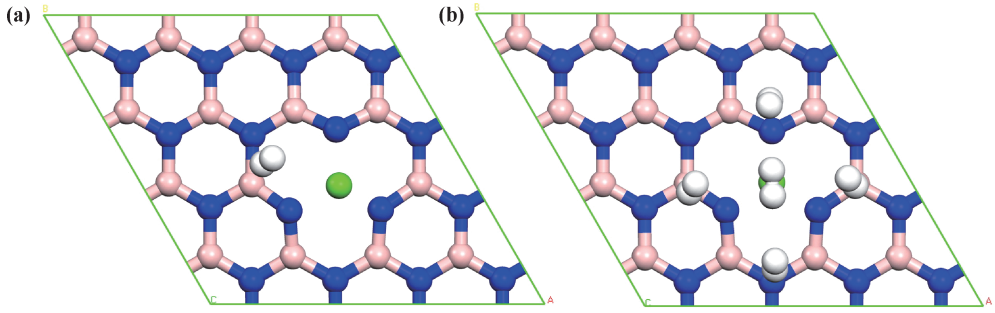


Fig. 7 Optimized structures of **(a)** one H_2 and **(b)** five H_2 molecules absorbed onto Ca–BN nanosheets with V_B.

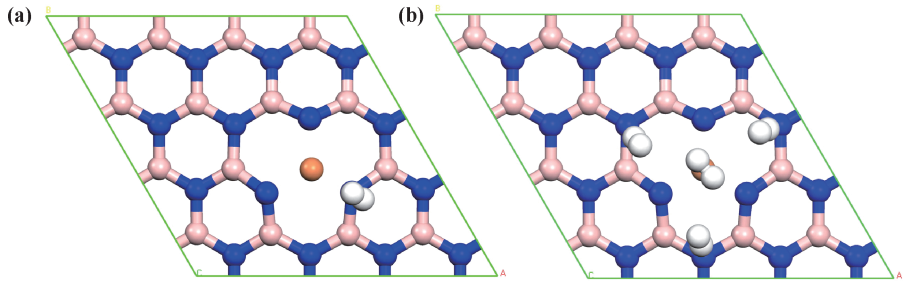


Fig. 8 Optimized structures of **(a)** one H_2 and **(b)** four H_2 molecules absorbed onto Sc-decorated BN nanosheets with V_B.

the adsorption energies significantly larger than those of typical vdW force but much smaller than those of metal hydrides. The larger adsorption energies result from the Kubas interaction [55]. The σ electrons of H_2 are transferred to the empty d orbitals of Sc atoms. At the same time, some filled d orbitals donate its electrons back to σ^* antibonding orbital of H_2 to form back–donation bonds. The back–donation bond is crucial for H_2 adsorption to Sc; the bond length of H_2 is enlongated, and the degree of enlongation is related to the intensity of the back–donation bonds. If transition metals donate enough electrons to the σ^* antibonding orbital, the H–H bond will be even dissociated.

As four H_2 molecules are adsorbed onto Sc-decorated BN nanosheets, the optimized H–H bond length is 0.76 Å, and the average bond length between H_2 and Sc is about 2.76 Å (Fig. 8). The binding energy is slightly reduced to –0.1 eV/H_2 at GGA and –0.26 eV/H_2 at LDA. When more hydrogen molecules are added onto Sc atoms, there are not enough electrons that can back donate to the antibonding orbital of H_2 to destabilize H_2, and the Kubas interaction is weakened correspondingly. The gravimetric density of hydrogen storage is estimated as ∼6 wt% if Sc atoms are placed on both sides of a 2×2 supercell of BN nanosheet with a B vacancy. The principles disclosed in this work may guide the future material design for hydrogen storage.

4 Conclusions

In summary, we have investigated the hydrogen adsorption in metal-decorated defective BN nanosheets by means of first-principles computations. The effects of vacancies are investigated on the binding of metal atoms to BN nanosheets. The binding energies of Ca and Sc on pristine BN nanosheets are far lower than the cohesive energies of the corresponding bulk metals; therefore, Ca and Sc atoms tend to form clusters on the surface of pristine BN nanosheets. Although the binding of metal atoms on nitrogen vacancies of BN nanosheets is enhanced, the binding energies are still smaller than the cohesive energies of the bulk metals, and then, Ca and Sc atoms persist in clustering on BN nanosheets with N vacancies. The situation changes in the case of BN nanosheets with B vacancies; the binding energies of Ca and Sc atoms on boron vacancies are much larger than the cohesive energies of the bulk Ca and Sc metals, and Ca and Sc atoms do not cluster on the BN nanosheets with B vacancies. Boron vacancies efficiently avoid the clustering problems due to charge transfer between metal atoms and BN substrates.

When hydrogen molecules are placed onto the vacancies of BN nanosheets, molecular hydrogen dissociates into hydrogen atoms to form chemical bonds with the atoms around the vacancy. However, as we place hydrogen molecules onto Ca or Sc decorated BN nanosheets with vacancies, the nondissociative hydrogen binding is achieved, and the intermediate hydrogen adsorption energy is obtained. Sc decorated BN nanosheets with boron vacancies demonstrate the optimal hydrogen adsorption characteristics in terms of the hydrogen adsorption energy up to –0.19∼–0.35 eV/H_2. The Kubas interaction is responsible for the enhanced hydrogen adsorption.

Metal atoms can bind tightly on BN nanosheets with experimentally available boron vacancies and avoid clustering problems. Metal-decorated defective BN nanosheets are promising hydrogen storage media.

Acknowledgements This study was supported by the Program for New Century Excellent Talents in University [NCET (08-0293)] in China.

References

1. R. Coontz and B. Hanson, Science, 2004, 305: 957
2. G. W. Crabtree, M. S. Dresselhaus, and M. V. Buchanan, Phys. Today, 2004, 57: 39
3. L. Schlapbach and A. Zütel, Nature, 2001, 414: 353
4. S. Satyapal, J. Petrovic, C. Read, G. Thomas, and G. Ordaz, Catal. Today, 2007, 120: 246
5. J. Graetz, Chem. Soc. Rev., 2009, 38: 73
6. R. C. Lochan and M. Head-Gordon, Phys. Chem. Chem. Phys., 2006, 8: 1357
7. C. Liu, Y. Chen, C. Z. Wu, S. T. Xu, and H. M. Cheng, Carbon, 2010, 48: 452
8. Z. Zhou, X. P. Gao, J. Yan, and D. Y. Song, Carbon, 2006, 44: 939
9. S. A. Shevlin and Z. X. Guo, Chem. Soc. Rev., 2009, 38: 211

10. Y. F. Zhao, Y. H. Kim, A. C. Dillon, M. J. Heben, and S. B. Zhang, Phys. Rev. Lett., 2005, 94: 155504
11. T. Yildirim and S. Ciraci, Phys. Rev. Lett., 2005, 94: 175501
12. A. Rubio, J. L. Corkill, and M. L. Cohen, Phys. Rev. B, 1994, 49: 5081
13. N. G. Chopra, R. J. Luyken, K. Cherrey, V. H. Crespi, M. L. Cohen, S. G. Louie, and A. Zettl, Science, 1995, 269: 966
14. Z. Zhou and Y.F. Li, J. Comput. Theor. Nanosci., 2009, 6: 327
15. Z. Y. Yang, Y. F. Li, and Z. Zhou, Front. Phys. China, 2009, 4: 378
16. Y. F. Li, Z. Zhou, D. Golberg, Y. Bando, P. v. R. Schleyer, and Z. F. Chen, J. Phys. Chem. C, 2008, 112: 1365
17. Y. F. Li, Z. Zhou, and J. J. Zhao, Nanotechnology, 2008, 19: 015202
18. Y. F. Li, Z. Zhou, and J. J. Zhao, J. Chem. Phys., 2007, 127: 184705
19. Z. Zhou, J. J. Zhao, Z. F. Chen, X. P. Gao, T. Y. Yan, and P. v. R. Schleyer, J. Phys. Chem. B, 2006, 110: 13363
20. T. Oku, T. Hirano, M. Kuno, T. Kusunose, K. Niihara, and K. Suganuma, Mater. Sci. Eng. B, 2000, 74: 206
21. R. Z. Ma, Y. Bando, H. W. Zhu, T. Sato, C. L. Xu, and D. H. Wu, J. Am. Chem. Soc., 2002, 124: 7672
22. C. C. Tang, Y. Bando, X. X. Ding, S. R. Qi, and D. Golberg, J. Am. Chem. Soc., 2002, 124: 14550
23. T. Oku, M. Kuno, and I. Narita, J. Phys. Chem. Solids, 2004, 65: 549
24. J. J. Zhao, A. Buidum, J. Han, and J. P. Lu, Nanotechnology, 2002, 13: 195
25. W. Shi and J. K. Johnson, Phys. Rev. Lett., 2003, 91: 015504
26. A. Cruz, V. Bertin, E. Poulain, J. I. Benitez, and S. Castillo, J. Chem. Phys., 2004, 120: 6222
27. Y. Fukai, The Metal–Hydrogen System: Basic Bulk Properties, Berlin: Spinger-Verlag, 1993
28. X. J. Wu, J. L. Yang, and X. C. Zeng, J. Chem. Phys., 2006, 125: 044704
29. Q. Sun, Q. Wang, P. Jena, and Y. Kawazoe, J. Am. Chem. Soc., 2005, 127: 14582
30. P. O. Krasnov, F. Ding, A. K. Singh, and B. I. Yakobson, J. Phys. Chem. C, 2007, 111: 17977
31. D. Golberg, Y. Bando, Y. Huang, T. Terao, M. Mitome, C. C. Tang, and C. Y. Zhi, ACS Nano, 2010, 4: 2979
32. L. Song, L. J. Ci, H. Lu, P. B. Sorokin, C. H. Jin, J. Ni, A. G. Kvashnin, D. G. Kvashnin, J. Lou, B. I. Yakobson, and P. M. Ajayan, Nano Lett., 2010, 10: 3209
33. H. B. Zeng, C.Y. Zhi, Z. H. Zhang, X. L. Wei, X. B. Wang, W. L. Guo, Y. Bando, and D. Golberg, Nano Lett., 2010, 10: 5049
34. C. H. Park and S. G. Louie, Nano Lett., 2008, 8: 2200
35. X. F. Gao, Z. Zhou, Y. L. Zhao, S. Nagase, S. B. Zhang, and Z. F. Chen, J. Phys. Chem. C, 2008, 112: 12677
36. W. Chen, Y. F. Li, G. T. Yu, Z. Zhou, and Z. F. Chen, J. Chem. Theory Comput., 2009, 5: 3088
37. W. Chen, Y. F. Li, G. T. Yu, C. Z. Li, S. B. Zhang, Z. Zhou, and Z. F. Chen, J. Am. Chem. Soc., 2010, 132: 1699
38. G. Kresse and J. Furthmüller, Phys. Rev. B, 1996, 54: 11169
39. J. P. Perdew, J. A. Chevary, S. H. Vosko, K. A. Jackson, M. R. Pederson, D. J. Singh, and C. Fiolhais, Phys. Rev. B, 1992, 46: 6671
40. D. M. Ceperley and B. J. Alder, Phys. Rev. Lett., 1980, 45: 566
41. Y. H. Kim, Y. F. Zhao, A. Williamson, M. J. Heben, and S. B. Zhang, Phys. Rev. Lett., 2006, 96, 016102
42. Y. F. Li, Z. Zhou, P. W. Shen, S. B. Zhang, and Z. F. Chen, Nanotechnology, 2009, 20: 215701
43. C. G. Zhang, R. W. Zhang, Z. X. Wang, Z. Zhou, S. B. Zhang, and Z. F. Chen, Chem. Eur. J., 2009, 15: 5910
44. D. Vanderbilt, Phys. Rev. B, 1990, 41: 7892
45. G. Kim, S. H. Jhi, S. Lim, and N. Park, Appl. Phys. Lett., 2009, 94: 173102
46. S. Azevedo, J. R. Kaschny, C. M. C. de Castilho, and F. de Brito Mota, Nanotechnology, 2007, 18: 495707
47. C. Jin, F. Lin, K. Suenaga, and S. Iijima, Phys. Rev. Lett., 2009, 102: 195505
48. X. J. Wu, J. L. Yang, J. G. Hou, and Q. S. Zhu, J. Chem. Phys., 2006, 124: 054706
49. M. Yoon, S. Y. Yang, C. Hicke, E. Wang, D. Geohegan, and Z. Y. Zhang, Phys. Rev. Lett., 2008, 100: 206806
50. M. Li, Y. F. Li, Z. Zhou, P. W. Shen, and Z. F. Chen, Nano Lett., 2009, 9: 1944
51. Q. Wang, Q. Sun, P. Jena, and Y. Kawazoe, J. Chem. Theory Comput., 2009, 5: 374
52. X. B. Yang, R. Q. Zhang, and J. Ni, Phys. Rev. B, 2009, 79: 075431
53. H. Lee, J. Ihm, M. L. Cohen, and S. G. Louie, Phys. Rev. B, 2009, 80: 115412
54. G. F. Wu, J. L. Wang, X. Y. Zhang, and L. Y. Zhu, J. Phys. Chem. C, 2009, 113: 7052
55. G. J. Kubas, J. Organomet. Chem., 2001, 635: 37